The Predicted Spectrum and Singlet–Triplet Interaction of the Hypermetallic Molecule SrOSr

ARTICLE *in* THE JOURNAL OF PHYSICAL CHEMISTRY A · MARCH 2013

Impact Factor: 2.69 · DOI: 10.1021/jp310531s · Source: PubMed

THE JOURNAL OF PHYSICAL CHEMISTRY A

Article

pubs.acs.org/JPCA

The Predicted Spectrum and Singlet−Triplet Interaction of the Hypermetallic Molecule SrOSr

B. Ostojić,[†] Per Jensen,*[,‡] P. Schwerdtfeger,[§,⊥] and P. R. Bunker[∥,#]

[†]Institute of Chemistry, Technology and Metallurgy, University of Belgrade, Studentski trg 14-16, 11 000 Belgrade, Serbia

[‡]FB C − Physikalische und Theoretische Chemie, Bergische Universität, D-42097 Wuppertal, Germany

[§]Fachbereich Chemie, Philipps-Universität Marburg, Hans-Meerwein-Str., D-35032 Marburg, Germany

[∥]Fritz-Haber-Institut der Max-Planck-Gesellschaft, Faradayweg 4-6, D-14195 Berlin, Germany

ABSTRACT: In accordance with previous studies in our group on Be, Mg, and Ca hypermetallic oxides, we find that SrOSr has a linear $\tilde{X}^1\Sigma_g^+$ ground electronic state and a very low lying first excited $\tilde{a}^3\Sigma_u^+$ triplet electronic state. No gas-phase spectrum of this molecule has been assigned yet, and to encourage and assist in its discovery we present a complete ab initio simulation, with absolute intensities, of the infrared absorption spectrum for both electronic states. The three-dimensional potential energy surfaces and the electric dipole moment surfaces of the $\tilde{X}^1\Sigma_g^+$ and $\tilde{a}^3\Sigma_u^+$ electronic states are calculated using a multireference configuration interaction (MRCISD) approach in combination with internally contracted multireference perturbation theory (RS2C) based on complete active space self-consistent field (CASSCF) wave functions applying a Sadlej pVTZ basis set for both O and Sr and the Stuttgart relativistic small-core effective core potential for Sr. The infrared spectra are simulated using the MORBID program system. We also calculate vertical excitation energies and transition moments for several excited singlet and triplet electronic states in order to predict the positions and intensities of the most prominent singlet and triplet electronic absorption bands. Finally, for this heavy molecule, we calculate the singlet−triplet interaction matrix elements between close-lying vibronic levels of the $\tilde{X}$ and $\tilde{a}$ electronic states and find them to be very small.

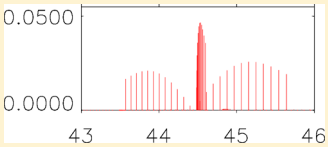

INTRODUCTION

The ratio of the electrostatic and gravitational forces between two electrons is about 10^{40}, and in 1937 Dirac[1] speculated that this value, which seems unreasonably large, could be a manifestation of the fact that the universe is very old. The currently accepted laws of physics depend on 25-odd parameters such as Planck's constant h, the gravitational constant G, and the mass m_e and charge $-e$ of the electron. If one assumes that these parameters − in particular G − vary with time, the ratio of the electromagnetic and gravitational interactions is then as large as 10^{40} simply because the universe has aged. It is indeed natural to ask whether the fundamental "constants" are really constant in time and space, and Dirac's ideas have given impetus to investigations of this problem that are continuing to the present day (for a recent review, see Uzan[2]). Generally, the possible variation of the fundamental parameters with time and space is not directly noticeable over the time span of typical human activities or over the spatial dimensions of the Earth, and one way of experimentally verifying such variations is to consider larger time spans and larger spatial dimensions, for example by observations involving celestial objects such as the measurement of the spectra of distant stars, searches for variations of planetary radii and moments of inertia, investigations of orbital evolution, and searches for anomalous luminosities of faint stars. However, direct laboratory measurements aimed at determining current variations of the fundamental constants are also possible, but the measurement techniques are clearly required to be of the highest possible precision.

It is well known that transition frequencies from spectroscopic experiments are some of the most accurately measured quantities known to mankind. Shelkovnikov et al.,[3] for example, have designed a spectroscopic experiment to investigate the time variation of the proton-to-electron mass ratio. In this experiment, a relative measurement precision of 2.2×10^{-14} was achieved. In another even more precise experiment, Rosenband et al.[4] determined the frequency ratio of two optical atomic clocks (based on optical transitions in single ions of aluminum and mercury, respectively) with a fractional uncertainty of 5.2×10^{-17} in order to estimate the time variation of the fine structure constant α.

In order that we can use spectroscopic experiments to investigate the possible time dependence of a fundamental parameter C, it is necessary that we measure a transition frequency ν that depends strongly on C so that $|\partial\nu/\partial C|$ is appreciably large. If this derivative is vanishingly small, we obviously cannot use ν to probe the time dependence of C. A molecule with a very small singlet−triplet splitting is likely to have singlet−triplet interaction that significantly influences at least some of its transition frequencies. Since the singlet−triplet interaction matrix elements depend on the fine structure

Special Issue: Oka Festschrift: Celebrating 45 Years of Astrochemistry

Received: October 24, 2012
Revised: March 16, 2013
Published: March 18, 2013

constant α, we can use measured values of these transition frequencies to probe the time dependence of α.[5,6] With the chief motivation of identifying molecules with transition frequencies particularly suitable for investigations of the possible time dependence of α and the proton-to-electron mass ratio, we have carried out a series of preliminary studies[7−9] predicting theoretically the spectra of the alkaline earth (Group 2) hypermetallic oxides Be_2O,[7] Mg_2O,[8] and Ca_2O,[9] which we expected to have small singlet−triplet splittings. We report here the continuation of this work for Sr_2O. No spectra of this molecule have been assigned yet, and we hope that our results will encourage and assist in their discovery. Long ago, strontium arc spectra were photographed by Gaydon,[10,11] who found some bands with intensities varying as the square of the Sr concentration. However, the positions of these bands do not accord with our predicted Sr_2O spectra. For all four of the M_2O molecules studied so far, we find that the ground electronic state is a linear symmetric singlet state ($\tilde{X}^1\Sigma_g^+$) and that there is a low-lying linear symmetric triplet state ($\tilde{a}^3\Sigma_u^+$). To estimate the spin−orbit interaction in Sr_2O, we calculate the spin−orbit matrix elements coupling the singlet and triplet electronic states.

Apart from the possible use for the investigation of the time dependence of fundamental parameters, there are other reasons for studying Group 2 M_2O molecules. They are examples of molecules having metal stoichiometries that exceed normal valence and as such are of interest from an electronic structure point of view. In practical terms the study of metal-rich clusters, both by spectroscopic investigation and by ab initio calculation, is important, particularly in the light of developing new catalytic materials. Moreover, the study of small clusters can help in understanding the emergence of crystalline properties from molecular properties. Of course, such theoretical results as ours must be supported by spectroscopic studies. For these molecules, modern high-resolution spectroscopic studies are few, and our work is very much directed toward predicting such spectra in the hope of encouraging activity in this area. Once such spectra have been obtained, we hope that our results will help in their analysis and assignment.

As described, and referenced in detail, in the following section, we first determine the three-dimensional potential energy surfaces, and the electric dipole moment surfaces, of the $\tilde{X}$ and $\tilde{a}$ electronic states using the CAS(15,28)-MRCISD+Q method in conjunction with second-order multireference perturbation theory (RS2C) and the Sadlej pVTZ basis set with the Stuttgart relativistic small-core effective core potential (ECP28MDF). In the third section of the paper, we describe the use of the calculated potential energy and dipole moment surfaces in a variational MORBID calculation to determine rovibrational term values and to simulate the infrared absorption spectrum of the two electronic states. We also calculate the vertical electronic energies and transition moments of several excited electronic states within both the singlet and triplet manifolds in order to determine the position and intensity of singlet and triplet electronic bands. These latter calculations have been carried out at the CAS(12,10)-MRCISD+Q/Sadlej-ECP28MDF level of theory. Further, we calculate the atomization energy and compare it with the mass-spectroscopic determination made by Drowart and colleagues.[12] Using the CAS(14,26)-MRCISD+Q method with the modified Sadlej pVTZ basis set and the Douglas−Kroll−Hess (DKH) Hamiltonian, we calculate the electronic matrix element between the singlet $\tilde{X}$ and triplet $\tilde{a}$ states for several geometries and then use our vibrational wave functions to determine the vibronic matrix elements between close-lying pairs of singlet ($\tilde{X}$) and triplet ($\tilde{a}$) vibronic states. These singlet−triplet perturbation matrix elements are reported at the end of the paper, and they turn out to be very small.

AB INITIO CALCULATION

Potential Energy and Dipole Moment Surfaces. We have computed the potential energy surfaces of the $\tilde{X}$ and $\tilde{a}$ electronic states of SrOSr by employing the complete active space (CASSCF) technique,[13,14] followed by a multireference configuration interaction (MRCI) treatment[15−17] in conjunction with a modified version of CASPT2 (Complete Active Space with Second-order Perturbation Theory) developed by Celani and Werner[18] and referred to as RS2C. The atomic orbital basis set employed for Sr and O was the Sadlej pVTZ basis set.[19,20] Strontium is heavy enough that relativistic effects are significant and therefore its inner shell electrons were replaced by a Stuttgart small-core relativistic effective core potential (ECP), ECP28MDF.[21]

As we found for BeOBe, MgOMg, and CaOCa, the description of the $\tilde{X}^1\Sigma_g^+$ ground electronic state of SrOSr requires a multiconfigurational treatment.[22] CASSCF calculations show that the two most important configurations of this state are represented by $|...\ 8\sigma_g^2\ 7\sigma_u^2\ 9\sigma_g^2\ 8\sigma_u^2\ 4\pi_u^4\ 4\pi_g^4\ 10\sigma_g^2\ 9\sigma_u^2\ 5\pi_u^4\ 11\sigma_g^2\rangle$ and $|...\ 5\pi_u^4\ 10\sigma_u^2\rangle$. At linearity, the coefficients in the CI expansion of these two dominant configurations are 0.72 and −0.60, respectively. In contrast, the $\tilde{a}^3\Sigma_u^+$ state is well described by a single-reference wave function: $|...\ 5\pi_u^4\ 11\sigma_g^1\ 10\sigma_u^1\ \rangle$ with a coefficient of 0.94 in the CI expansion.

We first examined the composition of the frontier, lower-, and higher-lying molecular orbitals in the ground electronic state of SrOSr. The $8\sigma_g$ and $7\sigma_u$ orbitals are mainly symmetric and antisymmetric linear combinations, respectively, of the 4s atomic orbitals on the two Sr centers. The $9\sigma_g$ orbital consists mainly of the oxygen 2s orbital, the $9\sigma_u$ orbital is mainly the oxygen $2p_z$ orbital directed along the molecular Z axis, and the $5\pi_u$ orbital consists mainly of the oxygen $2p_{x,y}$ orbitals perpendicular to the molecular axis. The molecular orbitals that involve the linear combinations of the 4p orbitals of Sr ($8\sigma_u$, $4\pi_u$, $4\pi_g$, and $10\sigma_g$) are placed energetically between the $9\sigma_g$ and $9\sigma_u$ molecular orbitals. This is different from the ordering of the molecular orbitals in MgOMg and CaOCa. The $8\sigma_u$ and $10\sigma_g$ orbitals are mainly composed of antisymmetric and symmetric linear combinations, respectively, of the strontium 4p orbitals directed along the molecular axis. The $4\pi_u$ and $4\pi_g$ orbitals are mainly symmetric and antisymmetric linear combinations, respectively, of the strontium $4p_{x,y}$ orbitals perpendicular to the molecular axis. The highest occupied molecular orbitals are the $11\sigma_g$ and $10\sigma_u$ orbitals. They are mainly symmetric and antisymmetric linear combinations, respectively, of the strontium 5s orbitals. The stability and strong bonding character of the $\tilde{X}$ and $\tilde{a}$ states in SrOSr arise from the predominantly ionic $Sr^+O^{2-}Sr^+$ nature of both states and bear a resemblance to the $\tilde{X}$ and $\tilde{a}$ states of the BeOBe, MgOMg, and CaOCa molecules.

Before adopting the active space for the calculations of the potential energy surfaces for the $\tilde{X}^1\Sigma_g^+$ and $\tilde{a}^3\Sigma_u^+$ electronic states, test calculations were carried out with different active spaces. It was found that the correct description of the ground electronic state and the first triplet electronic state of SrOSr requires the correlation of the core 4s and 4p electrons of the Sr atom. We chose the CASSCF active space, which consists of all configurations obtained by distributing the 28 electrons ($1s^22s^22p^4$ on O and $4s^24p^65s^2$ on each Sr) in 15 MOs (7−$11\sigma_g$, 7−$10\sigma_u$, 4−$5\pi_u$, and $4\pi_g$). Using the C_{2v} point group, the

dx.doi.org/10.1021/jp310531s | J. Phys. Chem. A 2013, 117, 9370−9379

Table 1. Vertical Singlet and Triplet Excitation Energies ΔE_{vert} (in cm^{-1}) of the Lowest Singlet and Triplet Excited States of SrOSr Calculated at the State-Average CAS(12,10)-MRCISD+Q/Sadlej-ECP28MDF Level of Theory[a]

singlet states						
state Φ[b]		configuration[c]	ΔE_{vert}[d]	$\lvert\langle\Phi\lvert\mu_x\rvert\tilde{X}\rangle\rvert$[e]	$\lvert\langle\Phi\lvert\mu_y\rvert\tilde{X}\rangle\rvert$[e]	$\lvert\langle\Phi\lvert\mu_z\rvert\tilde{X}\rangle\rvert$[e]
$\tilde{X}^1\Sigma_g^+$	1^1A_1	$0.74\ \lvert 5\pi_u^4\ 11\sigma_g^2\rangle - 0.56\ \lvert 5\pi_u^4\ 10\sigma_u^2\rangle$	0	0.0	0.0	0.0
$\tilde{A}^1\Sigma_u^+$	1^1B_2	$0.90\ \lvert 5\pi_u^4\ 11\sigma_g^1\ 10\sigma_u^1\rangle$	11391	0.0	1.17	0.0
$\tilde{B}^1\Sigma_g^+$	2^1A_1	$0.70\ \lvert 5\pi_u^4\ 10\sigma_u^2\rangle + 0.52\ \lvert 5\pi_u^4\ 11\sigma_g^2\rangle$	12910	0.0	0.0	0.0
$\tilde{C}^1\Pi_g$	1^1A_2	$0.89\ \lvert 5\pi_u^4\ 11\sigma_g^1\ 5\pi_g^1\rangle$	13337	0.0	0.0	0.0
	2^1B_2			0.0	0.0	0.0
$\tilde{D}^1\Pi_g$	2^1A_2	$0.91\ \lvert 5\pi_u^3\ 11\sigma_g^2\ 10\sigma_u^1\rangle$	27932	0.0	0.0	0.0
	3^1B_2			0.0	0.0	0.0
$\tilde{E}^1\Pi_u$	3^1A_1	$0.86\ \lvert 5\pi_u^4\ 10\sigma_u^1\ 5\pi_g^1\rangle$	14109	0.0	0.0	2.53
	1^1B_1			2.53	0.0	0.0
$\tilde{F}^1\Pi_u$	4^1A_1	$0.91\ \lvert 5\pi_u^3\ 11\sigma_g^1\ 10\sigma_u^2\rangle$	33297	0.0	0.0	0.49
	2^1B_1			0.49	0.0	0.0
triplet states						
state Φ[b]		configuration[c]	ΔE_{vert}[d]	$\lvert\langle\Phi\lvert\mu_x\rvert\tilde{a}\rangle\rvert$[e]	$\lvert\langle\Phi\lvert\mu_y\rvert\tilde{a}\rangle\rvert$[e]	$\lvert\langle\Phi\lvert\mu_z\rvert\tilde{a}\rangle\rvert$[e]
$\tilde{a}^3\Sigma_u^+$	1^3B_2	$0.93\ \lvert 5\pi_u^4\ 11\sigma_g^1\ 10\sigma_u^1\rangle$	0	0.0	0.0	0.0
$\tilde{b}^3\Pi_g$	1^3A_2	$0.92\ \lvert 5\pi_u^4\ 11\sigma_g^1\ 5\pi_g^1\rangle$	15701	2.94	0.0	0.0
	2^3B_2			0.0	0.0	2.94
$\tilde{c}^3\Pi_g$	2^3A_2	$0.92\ \lvert 5\pi_u^3\ 11\sigma_g^2\ 10\sigma_u^1\rangle$	27457	0.45	0.0	0.0
	3^3B_2			0.0	0.0	0.45
$\tilde{d}^3\Pi_u$	1^3A_1	$0.91\ \lvert 5\pi_u^4\ 10\sigma_u^1\ 5\pi_g^1\rangle$	16451	0.0	0.0	0.0
	1^3B_1			0.0	0.0	0.0
$\tilde{e}^3\Pi_u$	2^3A_1	$0.91\ \lvert 5\pi_u^3\ 11\sigma_g^1\ 10\sigma_u^2\rangle$	31967	0.0	0.0	0.0
	2^3B_1			0.0	0.0	0.0

[a]Calculations were carried out at the common singlet and triplet equilibrium geometries of ∠(SrOSr) = 180° and r(Sr−O) = 2.15 Å. [b]Symmetry labels are given for both the linear molecule (point group $D_{\infty h}$) and the bent molecule (point group C_{2v}). [c]Leading configurations of the CI eigenvector. [d]MRCISD values obtained using SA-CASSCF wave functions computed by averaging 11 singlet and 9 triplet states (relative to $\tilde{X}^1\Sigma_g^+$ for singlet states and to $\tilde{a}^3\Sigma_u^+$ for triplet states). [e]Matrix elements (in a.u.) of the x, y, and z components of the dipole moment between the state in question and the corresponding lower state ($\tilde{X}^1\Sigma_g^+$ for singlet states and $\tilde{a}^3\Sigma_u^+$ for triplet states) calculated at the state-average CAS(12,10)-MRCISD +Q/Sadlej-ECP28MDF level of theory. The y axis lies along the molecular axis.

active space consists of seven orbitals of A_1 symmetry, two of B_1 symmetry, five of B_2 symmetry, and one of A_2 symmetry; using the C_s point group, we have twelve orbitals of A' symmetry and three of A'' symmetry. For the singlet and triplet electronic states, we used the CASSCF state averaging (SA) procedure, that is, 1^1A_1 and 1^3B_2 in the C_{2v} group ($1^1A'$ and $1^3A'$ in the C_s group), and the two states were included with equal weights. The CI expansion of the CASSCF wave function starting from the CAS(15,28) orbitals was generated within the internally contracted method using single and double substitutions (MRCISD) from each reference determinant. In these MRCISD calculations all 28 valence electrons were correlated and the effect of higher excitations was taken into account by using the Davidson correction[23] (hereafter we denote this level of theory as CAS(15,28)-MRCISD+Q/Sadlej-ECP28MDF, and the corresponding energy as E_{MRCI}).

To account for core−valence correlation and to include the valence antibonding orbitals into the active space, it was necessary to perform two types of RS2C calculations, each using the CAS(15,28) wave functions as reference. In the first type (resulting in an energy which we designate as $E^{(1)}_{RS2C}$), the valence antibonding orbital of π_g symmetry ($5\pi_g$, given as an antisymmetric linear combination of the strontium $5p_{x,y}$ orbitals perpendicular to the molecular axis) was also correlated in the R2SC approach. The $5\pi_g$ orbital splits into a' and a'' molecular orbitals in C_s symmetry. Therefore, to the above-mentioned set of 12 MOs of A' symmetry one additional orbital of A' symmetry was added, and to the three MOs of A'' symmetry one orbital of A'' symmetry was added. In the second type of RS2C calculation (resulting in an energy denoted as $E^{(2)}_{RS2C}$), the $5\pi_g$ MO was not correlated in the RS2C approach. To avoid intruder state problems we applied an energy shift of 0.1 E_h and energies obtained in the RS2C calculations were corrected for this shift. Using these results, the energy values for the construction of the potential energy surfaces are given by

$$E = E_{MRCI} + E^{(1)}_{RS2C} - E^{(2)}_{RS2C} \quad (1)$$

The dipole moment surfaces for each electronic state were obtained, in the framework of C_s symmetry, at the CAS(15,28)-MRCISD/Sadlej-ECP28MDF level of theory. For the $\tilde{X}(\tilde{a})$ state, we calculated the energies and dipole moments at 55(56) geometries. The range of Sr−O bond lengths covered was between 2.00 and 2.35 Å, and the bond angle range was between 180 and 115°. The geometries were chosen such that energies up to 1500 cm^{-1} above the minimum of each state were covered with a uniform grid size. All electronic structure calculations were carried out using the MOLPRO 2010.1 suite of programs.[24]

Vertical Excitation Spectra of Low-Lying Excited States. The singlet and triplet vertical transition energies for several excited electronic states, at the common singlet and triplet equilibrium geometry of ∠(SrOSr) = 180° and r(Sr−O) = 2.15 Å (see the next section), were obtained in computations carried out in the framework of the D_{2h} and C_{2v} point groups. The closed orbital space in the CASSCF calculations involved nine orbitals: 7-9σ_g, 7-8σ_u, 4π_u, and 4π_g, while the 10-12σ_g, 9-11σ_u, 5-6π_u, and 5π_g MOs formed the active space. The CI expansion of

dx.doi.org/10.1021/jp310531s | J. Phys. Chem. A 2013, 117, 9370−9379

the CASSCF wave function starting from the CAS(12,10) orbitals was generated within the internally contracted method with single and double substitutions (MRCISD) from each reference determinant. In these MRCISD calculations all ten electrons were correlated and the effect of higher excitations was taken into account through the Davidson correction[23] (henceforth we denote this level of theory as CAS(12,10)-MRCISD +Q/Sadlej-ECP28MDF). The MRCISD values for the energies were obtained using SA-CASSCF wave functions computed by averaging eleven singlet states: two A_g, two B_{3u}, two B_{2u}, one B_{1u}, two B_{2g}, and two B_{3g} (i.e., four A_1, two B_1, three B_2, and two A_2 in the C_{2v} group); and nine triplet states: two B_{3u}, two B_{2u}, one B_{1u}, two B_{2g}, and two B_{3g} (i.e., two A_1, two B_1, three B_2, and two A_2 in the C_{2v} group). The vertical electronic energies and the leading configurations of the states (in $D_{\infty h}$ notation) are given in Table 1. The electronic transition moments are also given in Table 1; we give the absolute values of the transition moments for the components of the degenerate electronic states.

These results lead us to predict that there will be a strong electronic triplet state absorption band centered at about 640 nm and a strong electronic singlet state absorption band centered at about 710 nm. They do not agree well with the bands observed by Gaydon[10,11] at 595 and 605 nm in strontium arc spectra, although the bands have intensities that vary as the square of the Sr concentration. Gaydon suggested that the bands could be carried by the four-atomic molecule Sr_2O_2, and further investigations are required.

We have also calculated the atomization energy of SrOSr from the ground electronic state. We employed the energy of the SrOSr molecule in the ground electronic state at its equilibrium geometry ($\angle$(SrOSr) = 180°; r_e(Sr−O) = 2.15 Å) and the energy of SrOSr when both Sr atoms are at distances far away from the oxygen atom (15 and 20 Å) at the CAS(15,28)-MRCISD+Q/Sadlej-ECP28MDF level of theory. Our value of the atomization energy of 199.6 kcal/mol is in agreement with the experimental value of 194 ± 6 kcal/mol obtained from the mass spectrometric measurement reported by Drowart et al.[12]

MORBID CALCULATIONS

Rovibrational Calculations. From the ab initio calculations described in the preceding section we obtained for the $\tilde{X}$ and $\tilde{a}$ electronic states of SrOSr discrete values of the Born−Oppenheimer potential energies and dipole moment components at a grid of molecular geometries. In this section we report the result of using these data as input for simulations of the infrared spectra of SrOSr within these two electronic states. These simulations are carried out with the MORBID program system,[25−29] which is used for triatomic molecules to calculate rovibrational term values, transition wavenumbers, and spectral intensities; we refer the reader to the original papers[25−29] for details.

As the initial step of the MORBID calculations we require the analytical potential energy and dipole moment surfaces from ab initio data in order to interpolate and extrapolate our ab initio values. This is done by a least-squares fit to suitable parameterized functions of the ab initio values. These functions depend on the instantaneous internuclear distance displacements $\Delta r_{i2} = r_{i2} - r_{i2}^e$, i = 1 or 3, where r_{i2}^e is the equilibrium value of the distance r_{i2} between the "outer" strontium nucleus i = 1 or 3 and the "center" oxygen nucleus 2 and on the bond angle supplement $\bar{\rho} = \pi - \angle$(Sr−O−Sr). We use the following analytical expansion to represent the Born−Oppenheimer potential energy function:

$$V(\Delta r_{12}, \Delta r_{32}, \bar{\rho}) = \sum_{jkl} G_{jkl} y_1^j y_3^k (1 - \cos\bar{\rho})^l \quad (2)$$

with

$$y_i = 1 - \exp(-a_i \Delta r_{i2}) \quad (3)$$

The values of the expansion coefficients G_{jkl} in eq 2 were determined, together with the values of r_{i2}^e and of the molecular constants a_i in eq 3, for the $\tilde{X}$ and $\tilde{a}$ states in least-squares fits to the point-wise given ab initio energy surface. Here we took account of the fact that for a symmetric molecule like Sr_2O we have $a_3 = a_1$, $r_{32}^e = r_{12}^e$, and $G_{jkl} = G_{kjl}$, such that the function $V(\Delta r_{12},\Delta r_{32},\bar{\rho})$ is invariant under the interchange of Δr_{12} and Δr_{32}. The fitted parameters are listed in Table 2. The G_{jkl} parameters not given in this table were determined statistically to be insignificantly different from zero. The standard deviations of the least-squares fittings were 9.5 and 5.0 cm^{-1} for the $\tilde{X}$ and $\tilde{a}$ states, respectively. The energy at the minimum of the $\tilde{X}$ state was determined to be −135.923659 E_h and $T_e(\tilde{a})$ was obtained as 327 cm^{-1}. The latter is within the accuracy of our ab initio procedure.

Table 2. Potential Energy Parameters of $\tilde{X}^1\Sigma_g^+$ and $\tilde{a}^3\Sigma_u^+$ SrOSr Obtained by Fitting the Analytical Function of Equation 2 through the Calculated Ab Initio Energies[a]

	$\tilde{X}^1\Sigma_g^+$	$\tilde{a}^3\Sigma_u^+$
r_{12}^e/Å	2.14872(22)[b]	2.15271(12)
a_1/Å^{-1}	2.0[c]	2.0
G_{000}[d]/E_h	−135.923659(20)	−135.9221709(10)
G_{001}	524(34)	1444(17)
G_{002}	4598(53)	9029(29)
G_{101}	1273(104)	−89(54)
G_{102}	−3295(205)	−4858(108)
G_{200}	13919(87)	13943(46)
G_{201}	−1776(242)	−816(132)
G_{110}	2884(68)	3009(35)
G_{111}	−1657(1087)	−702(541)
G_{112}	8873(2156)	4199(1081)
G_{300}	4788(170)	4700(95)
G_{400}	2493(714)	2366(373)

[a]Units are cm^{-1} unless otherwise indicated. For SrOSr, $r_{32}^e = r_{12}^e$, $a_3 = a_1$, and $G_{jkl} = G_{kjl}$. [b]Quantities in parentheses are standard errors in units of the last digit given. [c]Parameters, for which no standard error is given, were held fixed in the least-squares fitting. [d]G_{000} is the potential energy value at equilibrium calculated as described here. In a comparable full-electron calculation, we obtained G_{000} = −6408.974546 E_h for the $\tilde{X}^1\Sigma_g^+$ state.

The components of the molecular dipole moment in the $\tilde{X}$ and $\tilde{a}$ electronic states of SrOSr are measured relative to the *xpq* axes defined in figure 1 of ref 26. The *xpq* axis system has its origin at the nuclear center of mass, and the p and q axes are in the plane defined by the three nuclei. The q axis bisects the bond angle $\angle$(Sr−O−Sr) and points so that the q coordinates of the "terminal" strontium nuclei 1 and 3 are positive. The p axis is perpendicular to the q axis and points so that the p coordinate of nucleus 3 is positive. In any electronic state of SrOSr, the x component of the molecular dipole moment $\bar{\mu}_x = \langle\Psi_{elec}|\mu_x|\Psi_{elec}\rangle_{el}$ vanishes by symmetry. Here, Ψ_{elec} is the electronic wave function of $\tilde{X}^1\Sigma_g^+$ or $\tilde{a}^3\Sigma_u^+$ SrOSr and the subscript "el" indicates that integration is over the electronic coordinates only. Consequently, we need only consider the p and q components $\bar{\mu}_p = \langle\Psi_{elec}|\mu_p|\Psi_{elec}\rangle_{el}$ and $\bar{\mu}_q = \langle\Psi_{elec}|\mu_q|\Psi_{elec}\rangle_{el}$,

dx.doi.org/10.1021/jp310531s | J. Phys. Chem. A 2013, 117, 9370−9379

respectively, and we represent these dipole moment components by the following analytical functions:

$$\bar{\mu}_q(\Delta r_{12}, \Delta r_{32}, \bar{\rho}) = \sin\bar{\rho} \sum_{jkl} \mu_{jkl}^{(q)} \Delta r_{12}^j \Delta r_{32}^k (1 - \cos\bar{\rho})^l \quad (4)$$

and

$$\bar{\mu}_p(\Delta r_{12}, \Delta r_{32}, \bar{\rho}) = \sum_{jkl} \mu_{jkl}^{(p)} \Delta r_{12}^j \Delta r_{32}^k (1 - \cos\bar{\rho})^l \quad (5)$$

where the $\mu_{jkl}^{(q)}$ and the $\mu_{jkl}^{(p)}$ are expansion coefficients. The two functions $\bar{\mu}_q(\Delta r_{12},\Delta r_{13},\bar{\rho})$ and $\bar{\mu}_p(\Delta r_{12},\Delta r_{13},\bar{\rho})$ are invariant and antisymmetric, respectively, under the interchange of Δr_{12} and Δr_{32}. Thus, in eq 4 we have $\mu_{jkl}^{(q)} = \mu_{klj}^{(q)}$ whereas in eq 5 $\mu_{jkl}^{(p)} = -\mu_{klj}^{(p)}$. In particular, $\mu_{jjl}^{(p)} = 0$.

We determine the parameters $\mu_{jkl}^{(q)}$ and $\mu_{jkl}^{(p)}$ by fitting eqs 4 and 5 to the ab initio dipole moment values. We used 10(7) parameters to fit 55(56) $\bar{\mu}_q$ values for the $\tilde{X}(\tilde{a})$ state with a standard deviation of 0.0023(0.0035) D. We used 8(8) parameters to fit the 38(40) $\bar{\mu}_p$ values for the $\tilde{X}(\tilde{a})$ state with a standard deviation of 0.0038(0.0029) D. In Table 3 we give the values obtained for the dipole moment parameters.

Table 3. Electric Dipole Moment Parameters of $\tilde{X}^1\Sigma_g^+$ and $\tilde{a}^3\Sigma_u^+$ SrOSr Obtained by Fitting the Analytical Functions of Equations 4 and 5 through the Calculated Ab Initio Values

		$\tilde{X}^1\Sigma_g^+$	$\tilde{a}^3\Sigma_u^+$
$\bar{\mu}_p$	μ_{100}/D Å^{-1}	−7.259(13)[a]	−7.6069(99)
	μ_{101}/D Å^{-1}	11.930(25)	10.136(18)
	μ_{102}/D Å^{-1}	10.1(15)	5.0(11)
	μ_{103}/D Å^{-1}	11.9(21)	18.6(16)
	μ_{200}/D Å^{-2}	−1.406(59)	−0.603(44)
	μ_{201}/D Å^{-2}	−17.19(95)	−11.44(80)
	μ_{202}/D Å^{-2}	−15.9(22)	−26.8(18)
	μ_{300}/D Å^{-3}	4.14(56)	2.50(43)
$\bar{\mu}_q$	μ_{000}/D Å	−0.3925(44)	−0.2502(49)
	μ_{001}/D Å	−1.445(24)	−0.730(31)
	μ_{002}/D Å	2.816(32)	2.928(48)
	μ_{100}/D Å^{-1}	3.244(16)	2.921(16)
	μ_{101}/D Å^{-1}		−1.552(45)
	μ_{102}/D Å^{-1}	−1.328(50)	
	μ_{200}/D Å^{-2}	−3.74(18)	−1.58(12)
	μ_{201}/D Å^{-2}	4.22(45)	
	μ_{110}/D Å^{-2}	6.50(20)	6.72(15)
	μ_{111}/D Å^{-2}	−1.76(55)	
	μ_{300}/D Å^{-3}	4.95(89)	

[a]Quantities in parentheses are standard errors in units of the last digit given.

Term Values and Spectral Simulations. We used the MORBID program system to calculate the rovibrational term values for the $\tilde{X}$ and $\tilde{a}$ electronic states of $^{88}Sr^{16}O^{88}Sr$. The lower $(J = l_2)$ rovibrational term values G_{vib} for the $\tilde{X}$ and $\tilde{a}$ electronic states are given in Table 4 together with the effective rotational constants B_{eff}. The values of G_{vib} and B_{eff} were obtained using the expression (for singlet states $N = J$)

$$E_{v,l_2}(N) = G_{vib} + B_{eff}[N(N+1) - l_2(l_2+1)] \quad (6)$$

for the two lowest MORBID-calculated term values in each vibrational state. For the $\tilde{a}$ electronic state, the effects of the nonzero electron spin were neglected.

The isotopes ^{88}Sr, ^{87}Sr, and ^{86}Sr have abundances of 83, 7, and 10%, respectively, and nuclear spins of 0, 9/2, and 0, respectively; the ^{18}O isotope has an abundance of 0.2%. In order to generate theoretical predictions for comparison with possible observed spectra, we have calculated with MORBID the term values of various isotopologues of Sr_2O, and the results are given in Table 5.

We have further used the MORBID program system to simulate the absorption spectra of $\tilde{X}^1\Sigma_g^+$ and $\tilde{a}^3\Sigma_u^+$ $^{88}Sr^{16}O^{88}Sr$ in the wavenumber region from 0 to 1000 cm^{-1}. The simulations were obtained separately for each electronic state for an absolute temperature $T = 15$ K and we included all states with J (N for the $\tilde{a}$ state) ≤ 25. The results are given in Figures 1 and 2. In these figures, each rotation−vibration transition is represented as a stick whose height is the integrated absorption coefficient $I(f \leftarrow i)$. The integrated absorption coefficient for an electric dipole transition from an initial state i (with energy E_i and rovibronic wave function ψ_i) to a final state f (with energy E_f and rovibronic wave function ψ_f) is given by[30]

$$I_{if} = \frac{8\pi^3 N_A \tilde{\nu}_{if} \exp\left(-\frac{E_i}{kT}\right)\left[1 - \exp\left(-\frac{hc\tilde{\nu}_{if}}{kT}\right)\right]}{3hcQ} \times S(f \leftarrow i) \quad (7)$$

where the partition function

$$Q = \sum_w g_w \exp(-E_w/kT) \quad (8)$$

with the summation running over all rovibronic states of the molecule, $S(f \leftarrow i)$ is the line strength of an electric dipole transition

$$S(f \leftarrow i) = g_{ns} \sum_{m_i,m_f} \sum_{A=X,Y,Z} |\langle\psi_f|\mu_A|\psi_i\rangle|^2 \quad (9)$$

g_{ns} is the nuclear spin statistical weight, $\tilde{\nu}_{if} = (E_f - E_i)/(hc)$ is the transition wavenumber, g_w is the total degeneracy of the state with the energy E_w, (μ_X, μ_Y, μ_Z) are the components of the molecular dipole moment operator in the space-fixed XYZ axis system, N_A is the Avogadro constant, k is the Boltzmann constant, h is Planck's constant, and c is the speed of light in vacuum. In eq 9, m_i and m_f are the projections, in units of $\hbar = h/(2\pi)$, of the angular momentum onto the space-fixed Z axis in the initial and final states, respectively.

SINGLET−TRIPLET INTERACTION

In Figure 3 we plot the lower vibronic term values for the $\tilde{X}$ and $\tilde{a}$ electronic states. At the bottom of the figure we give the symmetries of the rotational levels in each vibronic state for (even J/odd J) in the $\tilde{X}$ state, and for (even N/odd N) in the $\tilde{a}$ state (see figure (17-6) of ref 30). Singlet−triplet interaction will occur between singlet and triplet rotational levels having the same symmetry and J-value. In the triplet state, each rotational level N will be a triplet of levels having $J = N - 1$, N, and $N + 1$. Our calculations lead to the conclusion that among the low-lying $\tilde{X}$ and $\tilde{a}$ vibronic states the closest energy coincidence occurs for the $\tilde{X}$ state with $v_2^{l_2} = 7^1$ and the $\tilde{a}$ state with $v_2^{l_2} = 0^0$. To predict the strength of the singlet−triplet interaction between such a pair of rotational levels we have to perform ab initio calculations for the spin−orbit coupling matrix element.

Ab Initio Calculation of the Electronic Expectation Value $\langle\Psi_{elec}^{(\tilde{a})}|\hat{H}_{SO}|\Psi_{elec}^{(\tilde{X})}\rangle_{el}$. The off-diagonal matrix elements coupling $\tilde{X}$ and $\tilde{a}$ vibronic states in SrOSr arise from the spin−

dx.doi.org/10.1021/jp310531s | J. Phys. Chem. A 2013, 117, 9370−9379

Table 4. Calculated Vibrational Term Values $G_{vib} = E(v_1,v_2^{l_2},v_3,N_{min} = l_2) - E(0,0^0,0,0)$ and Effective Rotational Constants B_{eff} (in cm^{-1}) for $^{88}Sr^{16}O^{88}Sr$ in the Electronic States $\tilde{X}^1\Sigma_g^+$ and $\tilde{a}^3\Sigma_u^+$

$\tilde{X}^1\Sigma_g^+$				$\tilde{a}^3\Sigma_u^+$			
$(v_1,v_2^{l_2},v_3)$	N_{min}	G_{vib}	B_{eff}	$(v_1,v_2^{l_2},v_3)$	N_{min}	G_{vib}	B_{eff}
$(0,0^0,0)$	0	0.0[a]	0.0209	$(0,0^0,0)$	0	0.0[b]	0.0208
$(0,1^{1e,f},0)$	1	44.8	0.0211	$(0,1^{1e,f},0)$	1	64.2	0.0209
$(0,2^0,0)$	0	89.3	0.0213	$(0,2^0,0)$	0	128.2	0.0211
$(0,2^{2e,f},0)$	2	92.2	0.0213	$(0,2^{2e,f},0)$	2	131.1	0.0210
$(0,3^{1e,f},0)$	1	135.6	0.0214	$(0,3^{1e,f},0)$	1	192.2	0.0211
$(0,3^{3e,f},0)$	3	142.4	0.0215	$(0,3^{3e,f},0)$	3	200.9	0.0211
$(0,4^0,0)$	0	182.8	0.0216	$(1,0^0,0)$	0	221.3	0.0208
$(0,4^{2e,f},0)$	2	184.9	0.0216	$(0,4^0,0)$	0	260.6	0.0212
$(0,4^{4e,f},0)$	4	195.1	0.0216	$(0,4^{2e,f},0)$	2	260.6	0.0212
$(1,0^0,0)$	0	225.1	0.0209	$(0,4^{4e,f},0)$	4	273.5	0.0213
$(1,1^{1e,f},0)$	1	286.5	0.0210	$(1,1^{1e,f},0)$	1	302.3	0.0209
$(1,2^0,0)$	0	336.2	0.0212	$(1,2^0,0)$	0	370.1	0.0210
$(1,2^{2e,f},0)$	2	344.6	0.0212	$(1,2^{2e,f},0)$	2	377.7	0.0210
$(2,0^0,0)$	0	451.4	0.0212	$(2,0^0,0)$	0	440.3	0.0207
$(2,1^{1e,f},0)$	1	527.2	0.0211	$(2,1^{1e,f},0)$	1	541.0	0.0209
$(2,2^0,0)$	0	580.6	0.0212	$(2,2^0,0)$	0	611.2	0.0210
$(2,2^{2e,f},0)$	2	595.6	0.0212	$(2,2^{2e,f},0)$	2	626.3	0.0210
$(0,0^0,1)$	0	670.1	0.0208	$(0,0^0,1)$	0	671.2	0.0207
$(0,1^{1e,f},1)$	1	710.5	0.0210	$(0,1^{1e,f},1)$	1	731.7	0.0208
$(0,2^0,1)$	0	753.8	0.0212	$(0,2^0,1)$	0	796.2	0.0209
$(0,2^{2e,f},1)$	2	755.0	0.0212	$(0,2^{2e,f},1)$	2	796.8	0.0209
$(1,0^0,1)$	0	894.7	0.0208	$(1,0^0,1)$	0	891.5	0.0207

[a]Zero point energy is 487.4 cm^{-1}. [b]Zero point energy is 506.1 cm^{-1}.

Table 5. Vibrational Term Values (in cm^{-1}) of Various SrOSr Isotopologues

	$^{87}Sr^{16}O^{87}Sr$		$^{86}Sr^{16}O^{86}Sr$		$^{88}Sr^{18}O^{88}Sr$		$^{88}Sr^{16}O^{87}Sr$		$^{88}Sr^{16}O^{86}Sr$	
	$\tilde{X}$	$\tilde{a}$	$\tilde{X}$	$\tilde{a}$	$\tilde{X}$	$\tilde{a}$	$\tilde{X}$	$\tilde{a}$	$\tilde{X}$	$\tilde{a}$
ν_1	226	223	228	224	224	221	226	222	226	223
ν_2	45	64	45	64	42	60	45	64	45	64
ν_3	670	671	671	672	635	636	669	671	670	672
$2\nu_2$	89	128	89	128	84	121	89	128	89	128
$3\nu_2$	136	192	136	193	128	182	136	192	136	192
$\nu_1 + \nu_2$	288	303	289	304	279	294	287	303	288	303
$2\nu_1$	453	443	455	445	447	440	452	442	453	443
$2\nu_1 + \nu_2$	529	543	531	545	516	529	528	542	529	543
$\nu_2 + \nu_3$	711	732	711	732	673	693	711	732	711	732
$\nu_1 + \nu_3$	896	893	898	895	858	855	892	892	896	893

orbit interaction term $\hat{H}_{SO}$ in the total Hamiltonian. To calculate these off-diagonal vibronic matrix elements, we first have to determine the ab initio value of the one-electron integral $\langle\Psi_{elec}^{(\tilde{a})}|\hat{H}_{SO}|\Psi_{elec}^{(\tilde{X})}\rangle_{el}$, where $\Psi_{elec}^{(\tilde{X})}$ and $\Psi_{elec}^{(\tilde{a})}$ are the electronic wave functions of the $\tilde{X}$ and $\tilde{a}$ electronic states, respectively, and, as in the case of the electronic integrals $\bar{\mu}_p$ and $\bar{\mu}_q$ discussed above, the subscript "el" indicates that integration is taken over electronic coordinates only. The value of this integral will depend on the molecular geometry, and we calculate it by using an all-electron method that employs the second-order DKH Hamiltonian as incorporated in the MOLPRO 2010.1 program package, as the spin−orbit operator acts on the core-part of the valence orbitals which undergo spin−orbit splitting. The Sadlej pVTZ basis set was used for oxygen. For strontium, we used the Sadlej pVTZ basis set with s, p, and d functions decontracted to (18s,15p,10d) → [10s,7p,4d] with the addition of three f functions with exponents of 0.1094, 0.5408, and 1.3460, one g function with an exponent of 0.5408, and one extra hard p function with an exponent of 12 000.0. The active space in the CASSCF calculations consisted of all configurations obtained by distributing the 26 electrons in 14 MOs (8-11σ_g, 7-10σ_u, 4-5π_u, and 4π_g). In C_{2v} symmetry, the active space consists of six orbitals of A_1 symmetry, two of B_1 symmetry, five of B_2 symmetry, and one of A_2 symmetry. The CI approach was based on the SA-CASSCF procedure in which the singlet and triplet electronic states were included with equal weights. Starting from the CAS(14,26) orbitals, the CI expansion of the CASSCF wave function was generated within the internally contracted method with single and double substitutions (MRCISD) from each reference determinant. In these MRCISD calculations all 26 valence electrons were correlated and the effect of higher excitations was taken into account using the Davidson correction[23] (henceforth, we denote this level of theory as CAS(14,26)-MRCISD+Q/Sadlej* where * denotes the modified Sadlej pVTZ basis set).

dx.doi.org/10.1021/jp310531s | J. Phys. Chem. A 2013, 117, 9370−9379

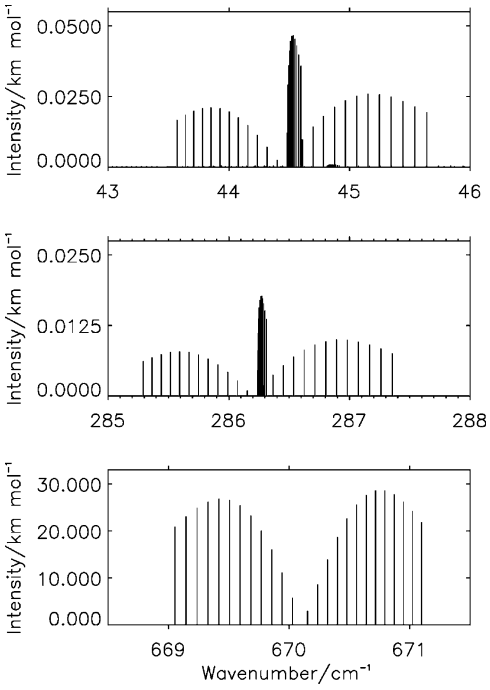

Figure 1. Predicted bands ν_2 (top panel), $\nu_1 + \nu_2$ (middle panel), and ν_3 (bottom panel) of $^{88}Sr^{16}O^{88}Sr$ in the $\tilde{X}^1\Sigma_g^+$ electronic state for $J \leq 25$ and $T = 15$ K. Note the very different ordinate scales of the three displays.

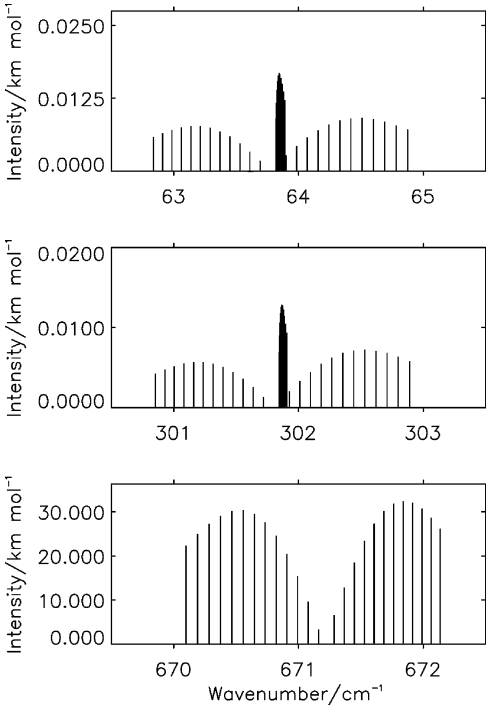

Figure 2. Predicted bands ν_2 (top panel), $\nu_1 + \nu_2$ (middle panel), and ν_3 (bottom panel) of $^{88}Sr^{16}O^{88}Sr$ in the $\tilde{a}^3\Sigma_u^+$ electronic state for $N \leq 25$ and $T = 15$ K. Note the very different ordinate scales of the three displays.

Spin−orbit coupling lifts the degeneracy of the electronic excited $^3\Sigma_u^+$ state; that is, in the $\Omega = \Lambda + M_S$ coupling scheme for the $D_{\infty h}$ point group the $^1\Sigma_g^+$ state reduces to 0_g^+ while the $^3\Sigma_u^+$ state splits into 0_u^- and 1_u components. Upon bending, that is, in the $\overline{C}_{2v}$ double group, the spin wave function in the singlet electronic state has A_1 symmetry, whereas the spin wave functions of the triplet electronic state have $A_2 \oplus B_1 \oplus B_2$

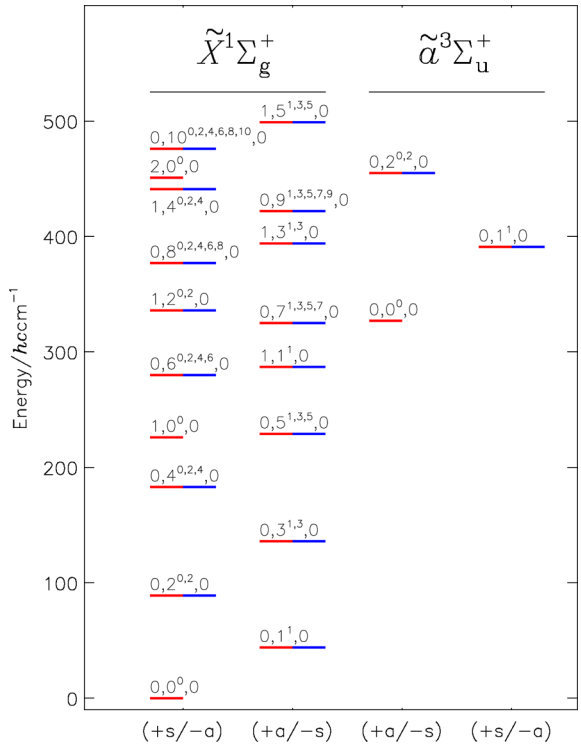

Figure 3. Lower vibronic states of $^{88}Sr^{16}O^{88}Sr$. At the bottom of the figure we give the symmetries of the rotational levels in each vibronic state for (even J/odd J) in the $\tilde{X}$ state and for (even N/odd N) in the $\tilde{a}$ state.

symmetry. The direct product representations of the space and spin functions are $A_1 \otimes A_1 = A_1$ for the singlet state and $B_2 \otimes A_2 = B_1$, $B_2 \otimes B_1 = A_2$, and $B_2 \otimes B_2 = A_1$ for the triplet state. So the overall symmetries of the electronic states involved show that there is a coupling between the A_1 state of the singlet state and the A_1 substate of the triplet state.

As stated above, the electronic integral $\langle \Psi_{elec}^{(\tilde{a})} | \hat{H}_{SO} | \Psi_{elec}^{(\tilde{X})} \rangle_{el}$ depends on the vibrational coordinates $(r_1, r_3, \overline{\rho})$. Since the stretching potentials of the $\tilde{X}$ and $\tilde{a}$ states are very similar, we only calculate the dependence of the integral on the bending coordinate. Thus, we have calculated values of $\langle \Psi_{elec}^{(\tilde{a})} | \hat{H}_{SO} | \Psi_{elec}^{(\tilde{X})} \rangle_{el}$ for ten values of the bond angle $\overline{\rho}$, with $r_1 = r_3 = 2.15$ Å fixed. Figure 4 shows that the spin−orbit splitting in the triplet excited stateincreases upon bending. The computed spin−orbit matrix elements $\langle \Psi_{elec}^{(\tilde{a})} | \hat{H}_{SO} | \Psi_{elec}^{(\tilde{X})} \rangle_{el}$ are displayed in Figure 5. In an ab initio calculation, the phase factors of the electronic wave functions vary with nuclear geometry in an arbitrary way, and in order to have consistent phase factors that vary smoothly with geometry we choose them such that the integral $\langle \Psi_{elec}^{(\tilde{a})} | \hat{H}_{SO} | \Psi_{elec}^{(\tilde{X})} \rangle_{el}$ is real and positive for all values of $\overline{\rho}$ considered. We have interpolated the discrete ab initio values of $\langle \Psi_{elec}^{(\tilde{a})} | \hat{H}_{SO} | \Psi_{elec}^{(\tilde{X})} \rangle_{el}$ with cubic splines and the resulting function is also plotted in Figure 5.

Vibrational Dependence of the Spin−Orbit-Interaction Matrix Elements. To calculate the off-diagonal matrix elements coupling the lower $\tilde{X}$ and $\tilde{a}$ vibronic states, we introduce the bending basis functions $\psi_{bend}^{(\sigma)}(\rho)$, where $\sigma = \tilde{a}(\tilde{X})$ for $\tilde{a}$-state($\tilde{X}$-state) bending functions. The functions $\psi_{bend}^{(\sigma)}(\rho)$ are obtained by Numerov−Cooley integration[31−33] in the course of the MORBID calculation;[25] they depend on the coordinate ρ which is almost, but not quite, equal to the bond angle supplement $\overline{\rho} = \pi - \angle(\text{Sr−O−Sr})$. We ignore the small

dx.doi.org/10.1021/jp310531s | J. Phys. Chem. A 2013, 117, 9370−9379

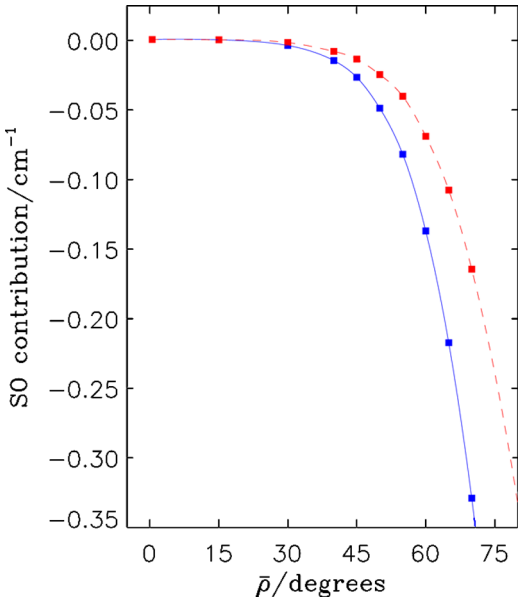

Figure 4. The difference between spin-free and relativistic singlet−triplet splittings as a function of $\bar{\rho} = 180° - \angle(\mathrm{Sr{-}O{-}Sr})$ calculated using the SA-CAS(14,26)-MRCISD+Q/Sadlej* method and the DKH Hamiltonian. The full line represents the difference between singlet−triplet splittings corresponding to the A_1 state of the singlet state and the A_1 substate of the triplet state. The dashed line represents the difference between singlet−triplet splittings corresponding to the A_1 state of the singlet state and the B_1 and A_2 substates of the triplet state; the B_1 and A_2 substates of the triplet state are degenerate.

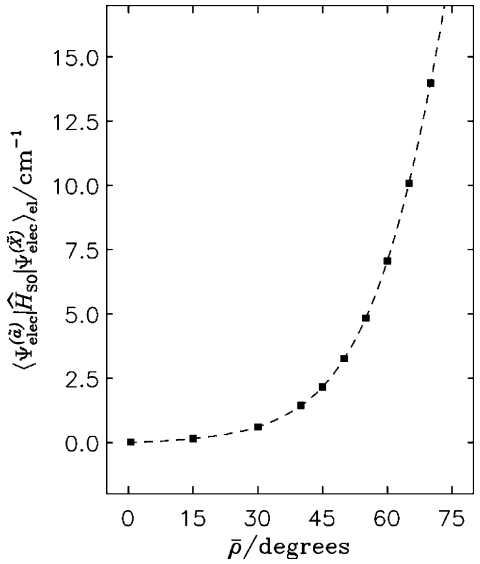

Figure 5. Values of $\langle\Psi^{(\tilde{a})}_{\mathrm{elec}}|\hat{H}_{\mathrm{SO}}|\Psi^{(\tilde{X})}_{\mathrm{elec}}\rangle_{\mathrm{el}}$ computed with MOLPRO for $r_1 = r_3 = 2.15$ Å are represented as filled squares. A cubic spline function determined to reproduce the ab initio values is plotted as a dashed curve.

difference between ρ and $\bar{\rho}$ here. Each bending function $\psi^{(\sigma)}_{\mathrm{bend}}(\rho)$ is characterized by values of the quantum numbers $v_2^{(\sigma)}$ and $l_2^{(\sigma)}$. We must calculate the bending integrals

$$\langle(v_2^{(\tilde{a})})^{l_2^{(\tilde{a})}}|\hat{H}_{\mathrm{SO}}|(v_2^{(\tilde{X})})^{l_2^{(\tilde{X})}}\rangle = \int_0^{\pi} \psi^{(\tilde{a})}_{\mathrm{bend}}(\rho)\langle\Psi^{(\tilde{a})}_{\mathrm{elec}}|\hat{H}_{\mathrm{SO}}|\Psi^{(\tilde{X})}_{\mathrm{elec}}\rangle_{\mathrm{el}}\psi^{(\tilde{X})}_{\mathrm{bend}}(\rho)\,\mathrm{d}\rho \quad (10)$$

where we have made use of the fact that the functions $\psi^{(\sigma)}_{\mathrm{bend}}(\rho)$ are all real. The integral on the right-hand side of eq 10 is calculated numerically with the values of the $\psi^{(\sigma)}_{\mathrm{bend}}(\rho)$ functions being obtained in MORBID calculations for the $\tilde{a}$ and $\tilde{X}$ states at identical grids of equidistantly spaced ρ-values and the values of $\langle\Psi^{(\tilde{a})}_{\mathrm{elec}}|\hat{H}_{\mathrm{SO}}|\Psi^{(\tilde{X})}_{\mathrm{elec}}\rangle_{\mathrm{el}}$ being calculated at these ρ-values from the cubic spline function plotted in Figure 5. The resulting values of $\langle(v_2^{(\tilde{a})})^{l_2^{(\tilde{a})}}|\hat{H}_{\mathrm{SO}}|(v_2^{(\tilde{X})})^{l_2^{(\tilde{X})}}\rangle$ with $|l_2^{(\tilde{a})} - l_2^{(\tilde{X})}| = |\Delta l_2| \leq 1$ are given in Table 6. The signs of the matrix elements result from the phase

Table 6. Bending Matrix Elements of the Spin−Orbit Interaction Operator (with $|l_2^{(\tilde{a})} - l_2^{(\tilde{X})}| \leq 1$, in cm^{-1}) Coupling the $\tilde{X}$ and $\tilde{a}$ Vibronic States Displayed in Figure 3

	$(v_2^{(\tilde{a})})^{l_2^{(\tilde{a})}}$			
$(v_2^{(\tilde{X})})^{l_2^{(\tilde{X})}}$	0^0	1^1	2^0	2^2
0^0	0.174	0.236	−0.199	
1^1	0.193	0.298	−0.329	0.367
2^0	−0.077	−0.194	0.372	
2^2		0.304		0.406
3^1	0.017	−0.058	0.264	−0.171
3^3				0.401
4^0	−0.042	−0.047	−0.039	
4^2		0.050		−0.027
5^1	−0.012	−0.050	0.083	−0.066
5^3				0.088
6^0	−0.015	0.001	−0.066	
6^2		−0.008		−0.051
7^1	−0.010	−0.020	0.001	−0.008
7^3				0.000
8^0	−0.006	0.006	−0.031	
8^2		−0.010		−0.023
9^1	−0.006	−0.008	−0.010	0.003
9^3				−0.009
10^0	−0.002	0.005	−0.013	
10^2		−0.007		−0.009

factor sign choice made for the $\psi^{(\sigma)}_{\mathrm{bend}}(\rho)$ functions in the Numerov−Cooley integration of the MORBID calculation. This phase factor choice is such that the $\psi^{(\sigma)}_{\mathrm{bend}}(\rho)$ functions, which vanish at $\rho = 0$, have positive values in the range $0 < \rho < \rho_{\mathrm{first}}$, where $\psi^{(\sigma)}_{\mathrm{bend}}(\rho)$ has its first node at ρ_{first} (or $\rho_{\mathrm{first}} = \pi$ for wave functions with no nodes); see Figure 6 for two examples. In obtaining the values of $\langle(v_2^{(\tilde{a})})^{l_2^{(\tilde{a})}}|\hat{H}_{\mathrm{SO}}|(v_2^{(\tilde{X})})^{l_2^{(\tilde{X})}}\rangle$ we neglect the dependence of the electronic integral $\langle\Psi^{(\tilde{a})}_{\mathrm{elec}}|\hat{H}_{\mathrm{SO}}|\Psi^{(\tilde{X})}_{\mathrm{elec}}\rangle_{\mathrm{el}}$ on r_1 and r_3. In order to obtain estimates of the complete off-diagonal matrix elements coupling the lower $\tilde{X}$ and $\tilde{a}$ vibronic states, we must in principle multiply the quantities in Table 6 by the overlap integral of the stretching basis functions associated with the $\tilde{X}$ and $\tilde{a}$ states, respectively. Since the $\tilde{X}$ and $\tilde{a}$ states have closely similar stretching potentials, these overlap integrals are taken as unity if both $v_1^{(\tilde{a})} = v_1^{(\tilde{X})}$ and $v_3^{(\tilde{a})} = v_3^{(\tilde{X})}$ and as zero if $v_1^{(\tilde{a})} \neq v_1^{(\tilde{X})}$ and/or $v_3^{(\tilde{a})} \neq v_3^{(\tilde{X})}$.

The bending matrix elements in Table 6 attain their largest absolute values, in the range from 0.1 to 0.5 cm^{-1}, for $|v_3^{(\tilde{a})} - v_3^{(\tilde{X})}| \leq 1$. The corresponding basis states, however, are separated by energy differences larger than 300 cm^{-1} (Figure 3) and so the energy shift due to spin−orbit interaction for these states can be estimated by second-order perturbation theory as being smaller than $(0.5\ \mathrm{cm}^{-1})^2/(300\ \mathrm{cm}^{-1}) \approx 0.001\ \mathrm{cm}^{-1}$. As mentioned

dx.doi.org/10.1021/jp310531s | J. Phys. Chem. A 2013, 117, 9370−9379

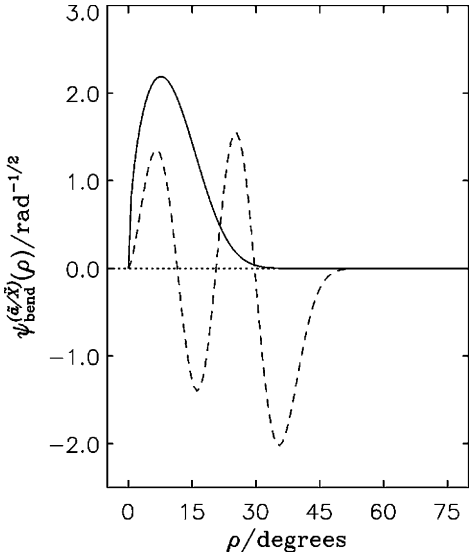

Figure 6. Solid curve: The bending basis function $\psi_{bend}^{(\tilde{a})}(\rho)$ with $(v_2^{(\tilde{a})})^{l_2^{(a)}} = 0^0$. Dashed curve: The bending basis function $\psi_{bend}^{(\tilde{X})}(\rho)$ with $(v_2^{(\tilde{X})})^{l_2^{(\tilde{X})}} = 7^1$.

above, the two levels in Figure 3 with the smallest energy separation have $(v_2^{(\tilde{a})})^{l_2^{(a)}} = 7^1$ and $(v_2^{(\tilde{X})})^{l_2^{(\tilde{X})}} = 0^0$, respectively; they are separated by about 2 cm^{-1} and coupled (Table 6) by a matrix element of −0.010 cm^{-1}. Thus the energy shift due to spin−orbit interaction can be estimated as $(-0.010\ \text{cm}^{-1})^2/(2\ \text{cm}^{-1}) \approx 0.00005\ \text{cm}^{-1}$. The small magnitude of the matrix element connecting the $(v_2^{(\tilde{a})})^{l_2^{(a)}} = 7^1$ and $(v_2^{(\tilde{X})})^{l_2^{(\tilde{X})}} = 0^0$ states can be understood by considering the bending basis functions in these two states; they are plotted in Figure 6.

SUMMARY AND CONCLUSION

By performing ab initio calculations we have found that the $\tilde{X}$ ground electronic state of Sr_2O has a linear SrOSr equilibrium structure of symmetry $^1\Sigma_g^+$. We have further found that the molecule has a very low lying triplet $\tilde{a}$ excited electronic state of symmetry $^3\Sigma_u^+$ and a singlet−triplet splitting, $T_e(\tilde{a})$, of 327 cm^{-1}.

We have calculated the three-dimensional potential energy surfaces, and the electric dipole moment surfaces, of the $\tilde{X}$ and $\tilde{a}$ states of SrOSr. We have used these surfaces in a variational MORBID calculation, to determine rovibrational term values and to simulate the infrared absorption spectrum of the two states. We have further calculated the vertical electronic energies and transition moments of several excited electronic states within both the singlet and triplet manifolds in order to determine the position and intensity of singlet and triplet electronic bands. We see from our results that no rovibrational or electronic spectra of SrOSr have been reported in the literature, and we hope our predictions will encourage and assist the discovery of such spectra. Using the CAS(14,26)-MRCISD+Q method with the modified Sadlej pVTZ basis set and the DKH Hamiltonian, we have calculated the electronic spin−orbit matrix element between the singlet $\tilde{X}$ and triplet $\tilde{a}$ electronic states for several geometries. We have then used our vibrational wave functions to determine the vibronic matrix elements between close-lying pairs of singlet and triplet vibronic states. These singlet−triplet perturbation matrix elements are reported at the end of the paper, and they turn out to be very small. In consequence, the transition frequencies in the SrOSr spectra involving the $\tilde{X}^1\Sigma_g^+$ and $\tilde{a}^3\Sigma_u^+$ electronic states are not influenced by singlet−triplet splitting to an extent that makes their measurement useful for an estimation of the possible time dependence of the fine structure constant α. We mentioned in the Introduction that the principal motivation of the present work and the preceding theoretical studies[7−9] is the identification of molecules with transition frequencies particularly suitable for investigations of the possible time dependence of the fine structure constant α and the proton-to-electron mass ratio m_p/m_e. In particular, we are hoping to identify transition frequencies strongly influenced by α through singlet−triplet interaction involving a small singlet−triplet splitting. For the molecules BeOBe,[7] MgOMg,[8] CaOCa,[9] and SrOSr studied thus far, the results have been somewhat disappointing in that all these molecules turned out to have singlet−triplet splittings larger than hoped for with correspondingly weak singlet−triplet interactions. We intend to continue investigating likely candidates such as BaOBa and it is our aim eventually to make theoretical predictions of transition frequencies as functions of α and m_p/m_e.

AUTHOR INFORMATION

Corresponding Author

*E-mail: jensen@uni-wuppertal.de.

Present Addresses

[⊥]P. Schwerdtfeger: Centre for Theoretical Chemistry and Physics (CTCP), The New Zealand Institute for Advanced Study (NZIAS), Massey University Auckland, Private Bag 102904, North Shore City, 0745 Auckland, New Zealand.

[#]P. R. Bunker: National Research Council of Canada, Ottawa, Ontario K1A0R6, Canada.

Notes

The authors declare no competing financial interest.

ACKNOWLEDGMENTS

B.O. gratefully acknowledges the financial support of the Ministry of Education and Science of Serbia (Contract No. 172001). P.S. is grateful to the Alexander von Humboldt Foundation for financial support of his stay at the Philipps University of Marburg. The work of P.J. is supported in part by the Deutsche Forschungsgemeinschaft and the Fonds der Chemischen Industrie. P.R.B. is grateful to the Fritz Haber Institute for hospitality.

REFERENCES

(1) Dirac, P. A. M. The Cosmological Constants. *Nature* **1937**, *139*, 323−323.

(2) Uzan, J.-P. Varying Constants, Gravitation and Cosmology. *Living Rev. Relativity* **2011**, *14*, 2−155. Online article cited January 22, 2013, http://www.livingreviews.org/lrr-2011-2.

(3) Shelkovnikov, A.; Butcher, R. J.; Chardonnet, C.; Amy-Klein, A. Stability of the Proton-to-Electron Mass Ratio. *Phys. Rev. Lett.* **2008**, *100*, 150801/1−4.

(4) Rosenband, T.; Hume, D. B.; Schmidt, P. O.; Chou, C. W.; Brusch, A.; Lorini, L.; Oskay, W. H.; Drullinger, R. E.; Fortier, T. M.; Stalnaker, J. E.; et al. Frequency Ratio of Al^+ and Hg^+ Single-Ion Optical Clocks; Metrology at the 17th Decimal Place. *Science* **2008**, *319*, 1808−1812.

(5) Uzan, J.-P. The Fundamental Constants and Their Variation: Observational and Theoretical Status. *Rev. Mod. Phys.* **2003**, *75*, 403−455.

(6) Beloy, K.; Hauser, A. W.; Borschevsky, A.; Flambaum, V. V.; Schwerdtfeger, P. Effect of α Variation on the Vibrational Spectrum of Sr_2. *Phys. Rev. A* **2011**, *84*, 062114/1−4.

(7) Ostojić, B.; Jensen, P.; Schwerdtfeger, P.; Assadollahzadeh, B.; Bunker, P. R. The Predicted Infrared Spectrum of the Hyperberyllium Molecule BeOBe in its $\tilde{X}^1\Sigma_g^+$ and $\tilde{a}^3\Sigma_u^+$ Electronic States. *J. Mol. Spectrosc.* **2010**, *263*, 21−26.
(8) Ostojić, B.; Bunker, P. R.; Schwerdtfeger, P.; Assadollahzadeh, B.; Jensen, P. The Predicted Spectrum of the Hypermetallic Molecule MgOMg. *Phys. Chem. Chem. Phys.* **2011**, *13*, 7546−7553.
(9) Ostojić, B.; Bunker, P. R.; Schwerdtfeger, P.; Gertych, A.; Jensen, P. The Predicted Infrared Spectrum of the Hypermetallic Molecule CaOCa in its Lowest Two Electronic States $\tilde{X}^1\Sigma_g^+$ and $\tilde{a}^3\Sigma_u^+$. *J. Mol. Struct.* **2012**, *1023*, 101−107.
(10) Charton, M.; Gaydon, A. G. Band Spectra Emitted by Strontium and Barium in Arcs and Flames. *Proc. Phys. Soc. A* **1956**, *69*, 520−526.
(11) Gaydon, A. G. Laboratory Production and Assignment of Spectra of Alkaline Earth Hydroxides and Oxides. *Mem. Soc. R. Sci. Liege, Collect. 4°* **1957**, *18*, 507−512.
(12) Drowart, J.; Exsteen, G.; Verhaegen, G. Mass Spectrometric Determination of the Dissociation Energy of the Molecules MgO, CaO, SrO and Sr_2O. *Trans Faraday Soc.* **1964**, *60*, 1920−1933.
(13) Werner, H.-J.; Knowles, P. J. A Second Order Multiconfiguration SCF Procedure with Optimum Convergence. *J. Chem. Phys.* **1985**, *82*, 5053−5063.
(14) Knowles, P. J.; Werner, H.-J. An Efficient 2nd-Order MC SCF Method for Long Configuration Expansions. *Chem. Phys. Lett.* **1985**, *115*, 259−267.
(15) Werner, H.-J.; Knowles, P. J. An Efficient Internally Contracted Multiconfiguration Reference Configuration Interaction Method. *J. Chem. Phys.* **1988**, *89*, 5803−5814.
(16) Knowles, P. J.; Werner, H.-J. An Efficient Method for the Evaluation of Coupling Coefficients in Configuration Interaction Calculations. *Chem. Phys. Lett.* **1988**, *145*, 514−522.
(17) Knowles, P. J.; Werner, H.-J. Internally Contracted Multi-Configuration Reference Configuration Interaction Calculations for Excited States. *Theor. Chim. Acta* **1992**, *84*, 95−103.
(18) Celani, P.; Werner, H.-J. Multireference Perturbation Theory for Large Restricted and Selected Active Space Reference Wave Functions. *J. Chem. Phys.* **2000**, *112*, 5546−5557.
(19) Sadlej, A. J. Medium-Size Polarized Basis Sets for High-Level Correlated Calculations of Molecular Electric Properties. *Collect. Czech. Chem. Commun.* **1988**, *53*, 1995−2016.
(20) Sadlej, A. J.; Urban, M. Medium-Size Polarized Basis Sets for High-Level-Correlated Calculations of Molecular Electric Properties: III. Alkali (Li, Na, K, Rb) and Alkaline-Earth (Be, Mg, Ca, Sr) Atoms. *J. Mol. Struct. (THEOCHEM)* **1991**, *234*, 147−171.
(21) Lim, I. S.; Stoll, H.; Schwerdtfeger, P. Relativistic Small-Core Energy-Consistent Pseudopotentials for the Alkaline-Earth Elements from Ca to Ra. *J. Chem. Phys.* **2006**, *124*, 034107/1−9.
(22) Boldyrev, A. I.; Shamovsky, I. L.; Schleyer, P. v. R. Ab Initio Prediction of the Structure and Stabilities of the Hypermagnesium Molecules: Mg_2O, Mg_3O and Mg_4O. *J. Am. Chem. Soc.* **1992**, *114*, 6469−6475.
(23) Langhoff, S. R.; Davidson, E. R. Configuration Interaction Calculations on the Nitrogen Molecule. *Int. J. Quantum Chem.* **1974**, *8*, 61−72.
(24) Werner, H.-J.; Knowles, P. J.; Knizia, G.; Manby, F. R.; Schütz, M.; Celani, P.; Korona, T.; Lindh, R.; Mitrushenkov, A.; Rauhut, G.; et al. *MOLPRO, version 2010.1, a package of ab initio programs*. See http://www.molpro.net.
(25) Jensen, P. A. New Morse Oscillator-Rigid Bender Internal Dynamics (MORBID) Hamiltonian for Triatomic Molecules. *J. Mol. Spectrosc.* **1988**, *128*, 478−501.
(26) Jensen, P. Calculation of Rotation-Vibration Line Strengths for Triatomic Molecules Using a Variational Approach. Application to the Fundamental Bands of CH_2. *J. Mol. Spectrosc.* **1988**, *132*, 429−457.
(27) Jensen, P. Hamiltonians for the Internal Dynamics of Triatomic Molecules. *J. Chem. Soc. Faraday Trans. 2* **1988**, *84*, 1315−1340.
(28) Jensen, P. Calculation of Molecular Rotation-Vibration Energies Directly from the Potential Energy Function. In *Methods in Computational Molecular Physics*; Wilson, S., Diercksen, G. H. F., Eds.; Plenum Press: New York, 1992.
(29) Jensen, P. The MORBID Method. In *Molecules in the Stellar Environment*; Jørgensen, U. G., Ed.; Lecture Notes in Physics *428*; Springer-Verlag: Berlin, 1994.
(30) Bunker, P. R.; Jensen, P. *Molecular Symmetry and Spectroscopy*, 2nd ed.; NRC Research Press: Ottawa, 2006. See http://www.nrcresearchpress.com/doi/book/10.1139/9780660196282.
(31) Numerov, B. Méthode Nouvelle de la Détermination des Orbites et le Calcul des Éphémérides en Tenant Compte des Perturbations [French with Summary in Russian]. *Trudy Glavnoi Rossiiskoi Astrofizicheskoj Observatorii* **1923**, *2*, 188−259.
(32) Cooley, J. W. An Improved Eigenvalue Corrector Formula for Solving the Schrödinger Equation for Central Fields. *Math. Comput.* **1961**, *15*, 363−374.
(33) Jensen, P. The Nonrigid Bender Hamiltonian for the Calculation of Rotation-Vibration Energies for a Triatomic Molecule. *Comput. Phys. Rep.* **1983**, *1*, 1−55.